BRIGHAM YOUNG UNIVERSITY

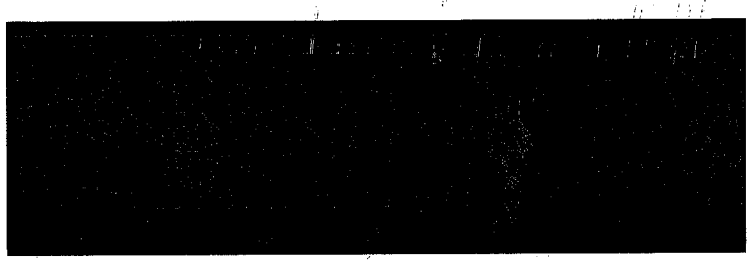

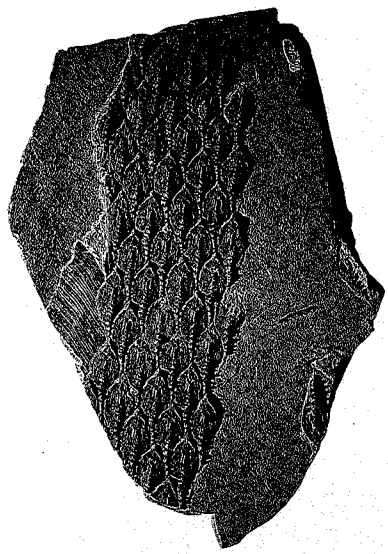

VOLUME 35 • 1988

BRIGHAM YOUNG UNIVERSITY GEOLOGY STUDIES

Volume 35, 1988

CONTENTS

A Publication of the
Department of Geology
Brigham Young University
Provo, Utah 84602

Editors
Bart J. Kowallis
Karen Seely

Brigham Young University Geology Studies is published by the Department of Geology. This publication consists of graduate student and faculty research within the department as well as papers submitted by outside contributors. Each article submitted by BYU faculty and outside contributors is externally reviewed by at least two qualified persons.

Cover: *Lepidodendron* sp. from the Manning Canyon Shale Formation. Donated by Gary Harris to the BYU paleobotanical lab.

ISSN 0068-1016
12-88 600 35388

Fault Kinematics and Paleostress Determined from Slickenlines in an Area of Unusual Fault Patterns, Southwestern Utah

ROBERT W. CLAYTON
Department of Geological Sciences, University of Southern California, University Park, Los Angeles, California 90089-0741

Thesis Chairman: BART J. KOWALLIS

ABSTRACT

Slickenline orientations were recorded from a 1500 km^2 area in southwestern Utah that contains complex fault geometries dominated by mixed north–south and east–west dip-slip and strike-slip faults. Eleven fault zones were thoroughly studied, from which 234 slickenline orientations were recorded. Four methods of determining paleostress were applied to the data and their results compared: Anderson (1951), Angelier (1979), Angelier and Mechler (1977), and Arthaud (1969). The results of these methods show a 135° clockwise rotation of the stress field during the Neogene from N–S extension 23–20 Ma., to NE–SW extension in mid-Miocene, to E–W extension post–mid-Miocene. An episode of NW–SE extension was also found, but its age is equivocal. The period of N–S extension, heretofore unrecognized in Basin and Range faulting, is also manifest in igneous dike orientations and depositional patterns of extrusive rocks. Its extent is as yet unknown, but it must be considered in future early Miocene tectonic models.

Agreement between the four paleostress methods depends on the degree of geometrical complexity of the fault set being analyzed. Anderson's (1951) method, which is applicable only to primary faults of demonstrable conjugate geometry, is nearly useless in the study area. Arthaud's (1969) method, which determines orientations of strain axes, is more useful because the axes' orientations are not limited to a specific angle from the faults. This advantage is lost, however, when total strain is not completely described by a fully three-dimensional fault system (i.e., "conjugate" faults are not present), and Andersonian conjugate faults must be assumed. The P-T dihedra and stress tensor methods are more widely applicable in the study area because they account for the fact that the slip direction on a given fault is determined by the relative magnitudes of the principal stresses; thus, they do not require stress axes to be oriented at a specific angle to the fault surface.

Careful fieldwork and the results of paleostress analyses show that lateral fault-block boundaries, or transfer (or accommodation) faults, are present in the study area at both the fault zone and regional scales. The Bible Spring fault zone (BSFZ) was a mid-Miocene transfer fault during the period of NE–SW extension as determined by its age, orientation, and paleostress analysis results. It is an example of a strike-slip fault active in a block-faulting extensional regime.

INTRODUCTION

Geologists have long been using the assumptions of Anderson (1951) to determine orientations of principal stresses from fault orientations. Until recently, however, it was not possible to analyze faults with oblique slip and groups of faults with complex geometries and obtain a solution with geologically plausible vertical and horizontal stress axes. Stress orientations are largely tectonically controlled, and are thus an important part of understanding regional tectonics. Since slickenlines (or slickenside striations) are records of past fault movements, their orientations can be useful in determining paleostresses (e.g., Anderson 1984, Anderson and Barnhard 1984, An-

A thesis submitted to the Department of Geology, Brigham Young University, in partial fulfillment of the requirements for the degree of Master of Science, March 1987.

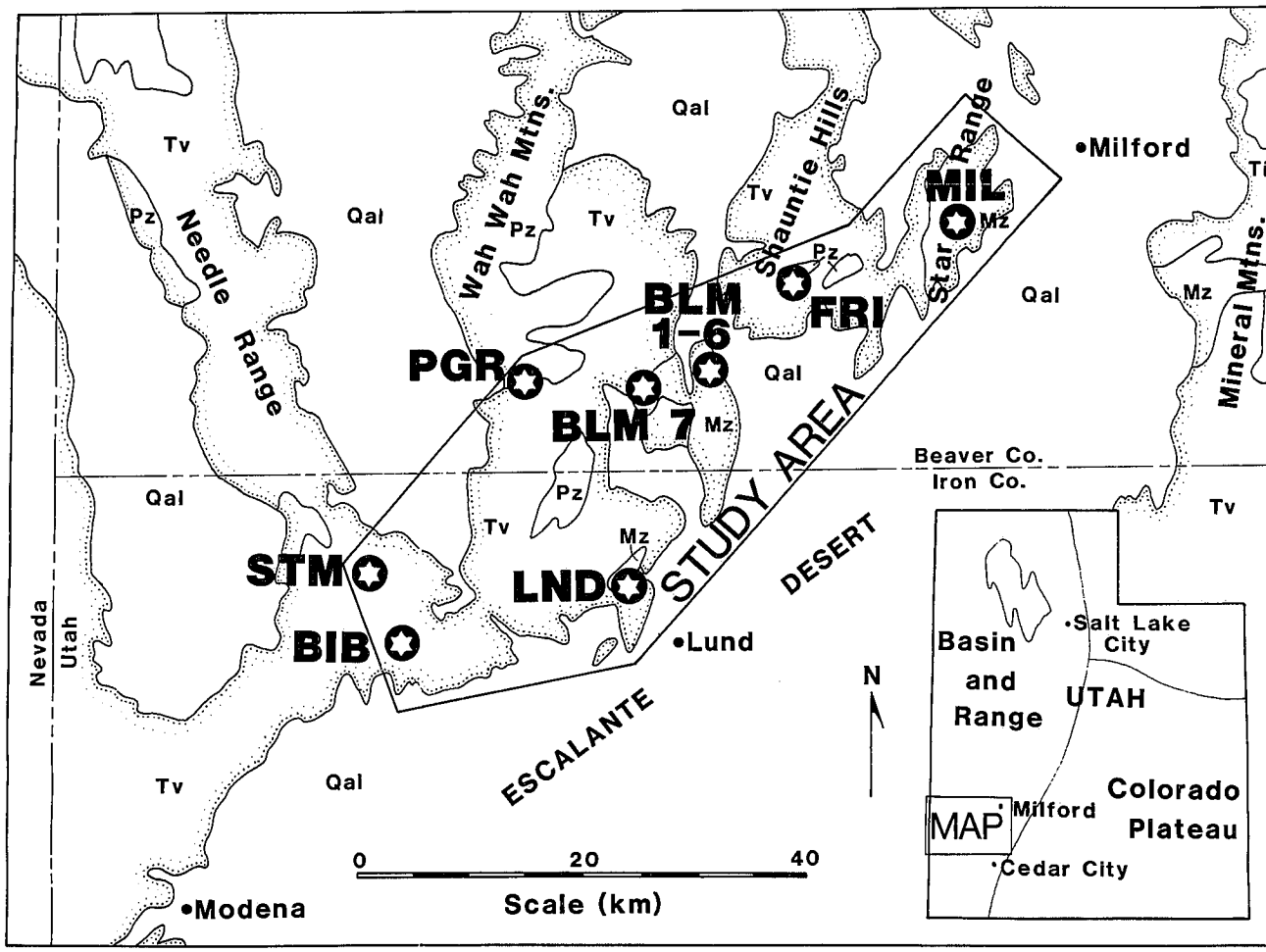

FIGURE 1.—*Index map of the study area. Bold letters indicate fault zone locations, named after the quadrangle maps on which they are located. BIB—Bible Spring; STM—Steamboat Mountain; BLM—Blue Mountain; LND—Lund; PGR—Pine Grove area; FRI—Frisco; MIL—Milford.*

gelier and others 1985). These paleostress orientations can then be used to constrain models of the tectonic evolution of the area.

The study area is part of the Oligocene to Miocene Pioche-Marysvale volcanic belt (Best and others 1984). Voluminous Oligocene calc-alkaline volcanism covered the tectonically quiet and topographically featureless eastern Great Basin. Less voluminous bimodal mafic-silicic Miocene volcanism was accompanied by block faulting beginning at 23 Ma. (Best and others 1984).

A belt of dip-slip and strike-slip faults occurs along a line of hills forming the northern edge of the Escalante Desert between Milford and Modena in southwestern Utah (fig. 1). It includes parts of (from east to west) the Star Range, Shauntie Hills, Wah Wah Mountains, and Needle Range. The area is approximately 75 km long and up to 25 km wide. It extends from the hills nearest Milford on the east to Bible Spring in the Needle Range on the west, and is bounded inclusively on the north by (from east to west in each mountain range) the Moscow Mine, White Mountain, Rose Spring Canyon, and Typhoid Spring. The belt of faults also marks the southern structural ends of three mountain ranges and three valleys. Baer (1962) postulated that in the Star Range, east–west faults are older than north–south faults. Orthogonal fault patterns also exist between the Star and Needle Ranges (Abbott and others 1983, Best and others in press, Best and others 1987, and Grant and Best 1979).

Paleostress analyses using faults and slickenlines have been made in nearby areas of the Basin and Range and Colorado Plateau transition zone. These studies used some of the same methods applied here. For example, Anderson (1984) showed that in some areas strike-slip and normal faults formed contemporaneously. Anderson and Barnhard (1984) detected north–south shortening in addition to east–west extension using the method of Angelier (1979). Barnhard and Anderson (1984) found a 45° clockwise rotation of the stress field during the Neogene

using slip-data analysis of slickenlines. Angelier and others (1985) used slickenlines to determine the timing of a 65° clockwise stress field rotation in the Lake Mead fault zone in southern Nevada during the Neogene. This thesis is one of the first published paleostress projects in the Basin and Range in Utah using slickenlines.

PROBLEM AND OBJECTIVES

The objective of this research was to determine changes in late Cenozoic stress field orientations in southwestern Utah by using slickenline and fault orientations. Fault patterns and preliminary field data (Abbott and others 1983, Best and others in press, Best and others 1987, and Grant and Best 1979) indicate a complex history of faulting, possibly including a rotation of the stress field and multiple faulting events. East–northeast-striking faults occur along the entire length of the study area, as do orthogonal mutually crosscutting sets of strike-slip and dip-slip faults that strike east–west and north–south. Fault patterns within ranges of the Great Basin are in general more complex than the patterns of range-bounding faults, but this is especially obvious in this area. These complex fault patterns preclude the determination of paleostress orientations solely from mapping, and demonstrate the need for detailed analysis of fault motions.

Angelier and others (1985) have shown the importance of slickenlines in resolving paleostress orientations where fault movements are oblique or of mixed type. Their method involves rigorous mathematical solution of stress tensors and calculation of the relative magnitudes of the principal stresses (see Angelier 1979, 1984). It was the aim of this research to use the method of Angelier (1979) to determine paleostress orientations in the study area and compare it to (a) the classical fault orientation approach of Anderson (1951), (b) the strain axis method of Arthaud (1969) as discussed by Bruhn and Pavlis (1981), and (c) the P-T dihedra method of Angelier and Mechler (1977) as discussed by Angelier (1984). These methods each place a different emphasis on slickenlines, so that a comparison of their results gives a measure of the importance of slickenlines in determining paleostress orientations.

In addition, the slip model of Reches (1983) was qualitatively tested to see if faults of the study area fit its predicted patterns. According to this theory, cogenetic faults should have orthorhombic symmetry.

FIELD METHODS

Slickenlines were most commonly found in sandstones, quartzites, silicified rocks, and along mapped faults, which were located using the maps referenced above. Slickenlines were not generally found in limestones except in fresh excavations, chert-rich beds, and silicified rocks. Similarly, unaltered volcanic rocks in the area were too weathered and intensely fractured to preserve slickenlines except in rare cases.

A total of 234 slickenlines were found and recorded in the field. At each location the following were recorded: (a) the strike and dip of each slickensided surface, (b) rake of slickenlines, (c) relative ages of slickenlines as determined from crosscutting relations, (d) sense of displacement on each slickensided surface and the degree of certainty with which this determination was made, (e) the approximate displacement on each slickenside surface and in the fault zone, (f) orientation of bedding (on a map), and (g) the location (on a map). This data formed the base of the paleostress analyses mentioned above. To determine the sense of displacement on slickensided surfaces, I used sense indicators as described by Angelier and others (1985) and as shown to me in the field by R. E. Anderson. These features included Riedel shears, corniced voids, rough facets, asymmetrical grooves, and dragged fragments.

METHODS OF PALEOSTRESS ANALYSIS

Four methods of paleostress analysis have been formulated by Anderson (1951), Angelier (1979), Angelier and Mechler (1977), and Arthaud (1969). All of these methods assume that faults form in conjugate pairs at some angle to the principal stress. They differ in how large that angle is, how tightly it can be constrained, and in the importance of the relative magnitudes of the principal stresses. All methods also assume that each group of faults formed in a single stress field, and that motion on each fault is independent of motion on other faults. Field observations, then, are very important in separating faults of different tectonic episodes and in identifying transfer faults, which cannot be analyzed by the above methods. Each of the methods are briefly described below.

Anderson (1951) assumes that conjugate faults form in pairs approximately 30° from the principal compressional stress (σ_1, where $\sigma_1 > \sigma_2 > \sigma_3$) and approximately 60° from the least compressive (extensional) stress (σ_3). The line of intersection of a conjugate pair of faults is defined as the direction of the intermediate stress (σ_2). Slickenlines should, therefore, be located 90° from σ_2 in the plane of the fault. This method, although supported by numerous laboratory experiments (for example, Paterson 1958), is simplistic in approach and fails to account for variables found in nature such as fault reactivation, oblique motions, mixed modes of faulting, and faults that do not occur with conjugate mates (see Angelier 1984). This method can not be accurately applied, then, to reactivated faults or those that do not have demonstrable Andersonian geometries, which includes most faults of this study. It is instructive, however, to do so to compare its

results with those of the other methods since many field geologists have assumed these relations in drawing conclusions about paleostress from mapped fault patterns. This practice will be shown to be highly unreliable.

Arthaud's (1969) method, as described by Bruhn and Pavlis (1981), has distinct advantages over Anderson's analysis. Since it makes no assumption concerning the angular relationship between the fault and principal stress axes, it is useful in analyzing structurally complex terranes where such restrictions are not practical. It is also equivalent to earthquake focal mechanism solutions, allowing comparisons of seismicity and recent faulting. If some conjugate geometries are not present in the data set, conjugate faults must be assumed to completely describe strain in three dimensions, and Arthaud's method loses its major advantage. In such cases, I have assumed with Bruhn and Pavlis (1981) Andersonian geometries.

Arthaud's method is different from the other methods described here because it finds orientations of strain axes. Stress axes are assumed to be roughly parallel to strain axes for comparison with other methods (σ_1 is the shortening direction, σ_3 the elongation direction). The axis of zero strain (M-pole, which is approximately parallel to σ_2) is the pole to a plane that contains the striation and the pole to the fault. This M-pole is equivalent to the B-axis of earthquake focal mechanism solutions. The other strain axis orientations are located as bisectors to the quadrants created by the intersection of conjugate faults. The shortening and extensional fields are distinguished on the basis of sense of slip on the fault system.

The P-T dihedra method of Angelier and Mechler (1977), as described by Angelier (1984), can be done easily on a stereo net. The fields of compression (P) and tension (T) are located by plotting the "accessory plane"—which is the plane whose pole is the fault striation—on a stereo net. The intersection of the accessory plane and the fault forms four quadrants, which are defined as P or T by sense of motion on the fault. P and T quadrant bisectors are not necessarily parallel to principle stress axes, but the axes usually plot within a few degrees (see Angelier 1984). This method does not require Andersonian conjugate mates for each fault, and restricts the orientation of principal stresses only by the extents of P and T quadrants. The justification for this apparent imprecision lies in the implicit fact that there is no constraint on the relative magnitudes of the principal stresses. For a given fault plane and slickenline, a number of stress orientations may account for their orientations depending on the relative magnitudes of the stresses (Bott 1959). McKenzie (1969) contends that for faults which form on pre-existing fractures, σ_1 and σ_3 may actually lie anywhere in the P and T quadrants. Raleigh and others (1972), however, state that only fractures whose poles are between 40° and 80° to σ_1 will slip, and that new fractures will form when favorable oriented fractures are not present. σ_1 and σ_3 orientations are constrained in this method by the combination of solutions for a group of related faults. Overlapping P and T quadrants of groups of faults are plotted in the figures that follow, and it is assumed that σ_1 and σ_3 lie in these overlap areas (Angelier 1984).

The method of Angelier (1979) is a stress tensor analysis computer program. It requires input of fault plane orientation, rake of striae, sense of displacement, a degree of certainty with which displacement determination was made, and a weight on a scale of 1 to 9 by displacement across the fault (larger faults are given more weight). Large-scale faults are more reliable stress indicators since small faults can be influenced by motions between large blocks (Zoback and Zoback 1980). The program then performs the P-T dihedra analysis for each fault and calculates a best-fit solution for the data set. Data in this study were grouped as fault zones.

The assumptions used in this method are the same as for the P-T dihedra method. The advantage lies, however, in the computation of ϕ (phi), the relative magnitude of the principal stresses, given by:

$$\sigma_4 = (\sigma_2 - \sigma_3) / (\sigma_1 - \sigma_3)$$

A phi value near zero indicates that σ_2 is almost equal in magnitude to σ_3; likewise, a value near 1 shows that σ_2 is like σ_1. ϕ is calculated from the slickenline orientation using a four-dimensional tensor analysis. The importance of ϕ is best seen in cases of oblique fault movement, since it is the relative magnitude of the intermediate stress that ultimately determines the direction of motion (Bott 1959). Orientations of the resolved shear stress on the fault surface, and hence displacement, shift along the fault plane away from σ_1 and toward σ_3 as ϕ increases from 0 to 1 (Angelier 1979). The advantages of this method are that oblique motions can be explained by more nearly horizontal and vertical stress axes than the other methods by computing an appropriate value of ϕ. Like all other methods, satisfactory results cannot be obtained for fault sets in which all faults are geometrically similar (Angelier 1979) since the total kinematic and strain solution is not completely described.

The slip model of Reches (1983) states that faults which form on planes of pre-existing weakness in a three-dimensional stress field form in three or four sets with orthorhombic symmetry and not in conjugate pairs. Conjugate faults form by plane strain, which, according to Reches, does not occur in nature. Some relevant problems with this model are (1) conjugate faults are very common in the field and (2) a fault system as complex as the one suggested would easily be masked by a complex stress history in which sets of faults are superimposed on each other. Orthorhombic fault sets would be found,

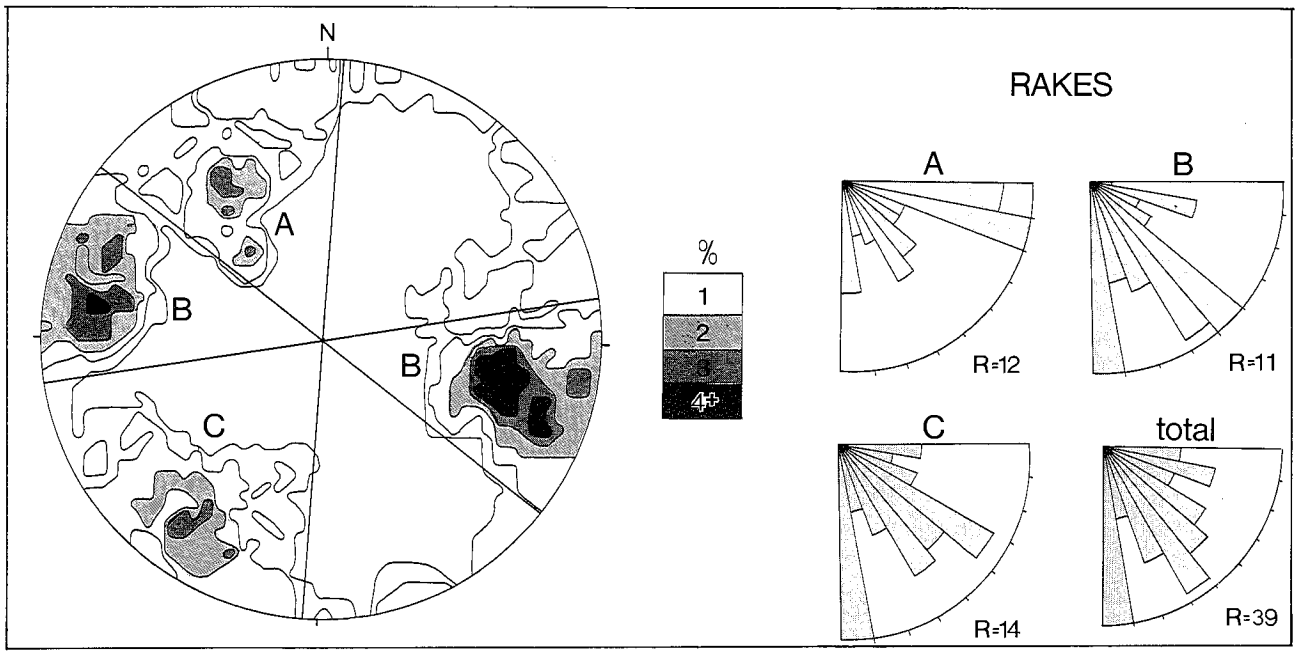

FIGURE 2.—*Lower hemisphere equal area projection of poles to fault planes for the entire data set. Rose diagrams indicate rake distributions for each of the three groups and for the entire data set. Radius values are shown.*

therefore, only in areas of simple stress history. This model was qualitatively compared with the data sets described below.

DATA ANALYSES

The 234 striation orientations recorded were divided into 8 geographical groups (fig. 1). Each of these groups is either a fault zone, group of fault zones, or faults in a restricted geographical area. In the course of stress analyses the data were further divided into a total of 15 groups based on coherency of stress analyses.

In figure 2, the faults are divided into three groups according to strike—group A strikes NE–SW, group B strikes N–S, and group C strikes NW–SE. As seen in the rose diagrams, NE–SW-striking faults are mostly strike slip and N–S-striking faults are mostly dip slip, but as a group the 234 faults make little sense. Note the abundance of oblique-slip faults in each group. From this diagram it is obvious that further subdivision of the data was necessary.

It must be emphasized here that the groups shown in figures 14 and 21 were demonstrated by careful field study to be transfer faults, which are not a primary product of a stress regime. Transfer faults are fault-block boundaries that strike roughly parallel to the extension direction. They may separate terranes of differing extension rate or mark a reversal of dip between subparallel or en echelon normal faults (Gibbs 1984, Lister and others 1986). They can range in size from centimeters (this paper) to the size of the Garlock Fault in southern California, which separates extended regions to the north from less extended areas to the south (Davis and Burchfiel 1973). Paleostress analysis of the Garlock or other transfer faults would be meaningless, since a basic assumption of paleostress analysis is that each fault slipped independent from motion on any other fault (Angelier 1984). The data in figures 14 and 21 are presented only for comparison of the various methods and because they show a common relationship between faults and apparent stresses.

Each of the 15 fault groups is discussed below. Group names refer to the abbreviations as used on the index map (fig. 1).

MIL GROUP

The MIL group consists of 11 strike-slip (fig. 3) and 14 dip-slip (fig. 4) faults recorded over a relatively large area in the Star Range. Strike-slip faults are generally oriented transverse to the north–south-striking dip-slip faults, and were thought by Baer (1962) to pre-date them. Anderson's method gives results inconsistent with those of the other methods for strike-slip faults. The reasons for these conflicting results are (1) the restriction of σ_2 to the intersection of conjugate fault planes, which is not true of the other methods, and (2) the presence of reactivated faults and/or significant deviatoric stress. In this case, then, Anderson's method does not give reliable results. Arthaud's method suffers similarly since so many of the strike-slip faults have low dips.

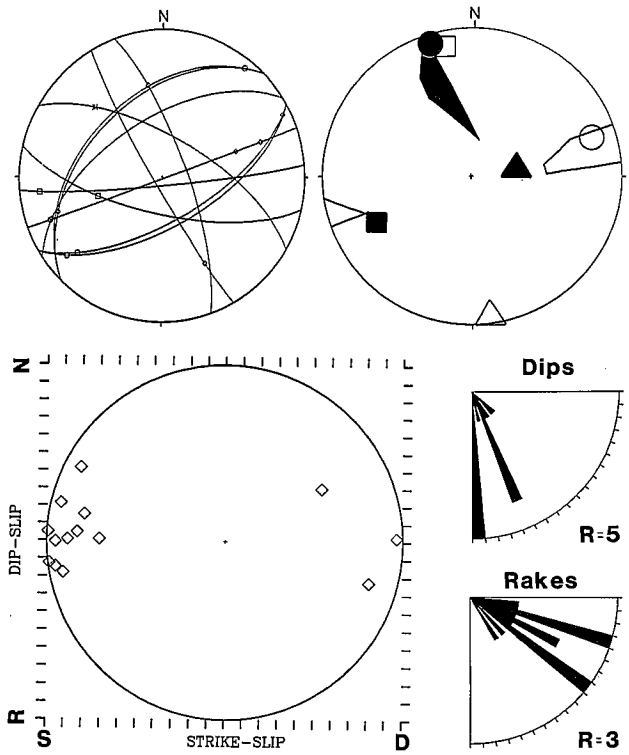

FIGURE 3.—*MIL strike-slip data. Upper left: Lower hemisphere equal area projection of faults and slickenlines. Squares and circles represent slickenlines of normal or dextral motion; asterisks are sinistral or reverse motion. Upper right: Results of four methods of paleostress analysis plotted on a lower-hemisphere equal-area projection. Triangles are Anderson's method; squares, Arthaud's method; circles, stress tensor method; irregular shapes, P-T dihedra method. Shaded shapes are* σ_1 *or compressional quadrants; open shapes are* σ_3 *or tensional quadrants. Lower left: Fault motion histogram. End members are labeled; R, reverse; N, normal; S, sinistral; D, dextral. Lower right: Rose diagrams for dip and rake distributions. Radius values are shown.*

The method of stress tensors and P-T dihedra method agree in placing σ_1 NNW–ESE and σ_3 ENE–WSW for strike-slip faults. The value of these methods in this case is their ability to deal with oblique rake angles and moderately dipping strike-slip faults.

MIL normal faults are much more straightforward (fig. 4). Each method places σ_1 near vertical and the extension direction (σ_3) near east–west, consistent with known Quaternary stress field orientations (Zoback and Zoback 1980). Normal and strike-slip faults, then, both formed in east–west extension, with the possible exception of the two normal faults that strike approximately 45° and 55°, respectively (see fig. 4). These two were recorded in the same fault zones as strike-slip faults of the same orientations, and may therefore represent older motions that pre-date the Quaternary stress field. Such orthogonal slickenlines are common (R. E. Anderson personal communication 1987), but no crosscutting relationships were observed to determine relative ages.

FRI GROUP

An interesting fault zone is located on the south side of White Mountain in the Shauntie Hills (fig. 5). The fault zone is approximately 125 meters long. Most of the 43 faults recorded here have slickenlines that plunge to the north (fig. 6). They fall into three main groups: NE-striking, SE-dipping; NW-striking, SW-dipping; and north-striking, steeply-dipping (fig. 7). The NE- and NW-striking faults appear to be a conjugate set of normal faults that have been tilted 40° to the south, and the steeply dipping faults strike N–S between them. The fault zone cuts Mississippian limestones whose bedding dips 15° to the south, so a palinspastic reconstruction to bring the intersection of these conjugate faults to horizontal is geologically impractical. The faults must be considered as approximately in place or tilted at most 15° to the north.

The slickensided fault zone terminates on the south against an east–west-striking, steeply dipping normal fault that juxtaposes 33-m.y.-old ash flow tuffs against the Mississippian limestones. Every slickenline in the zone

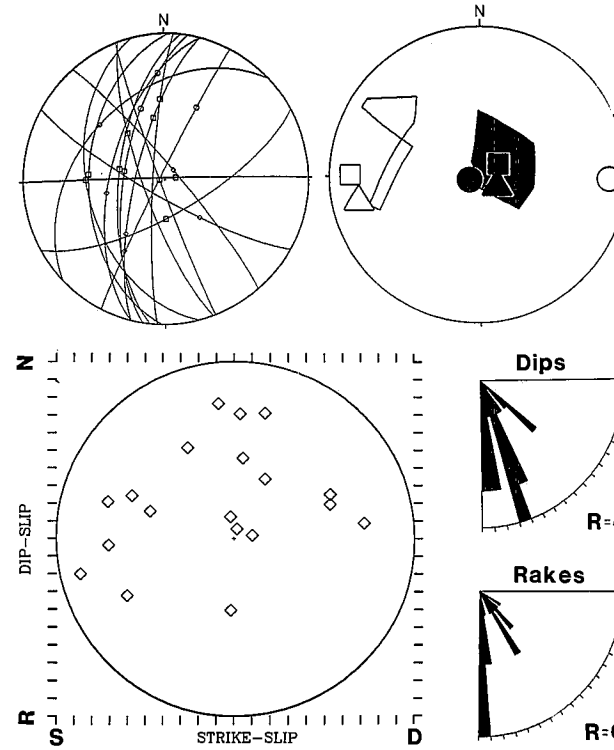

FIGURE 4.—*MIL dip-slip data. Figure 3 caption explains symbols.*

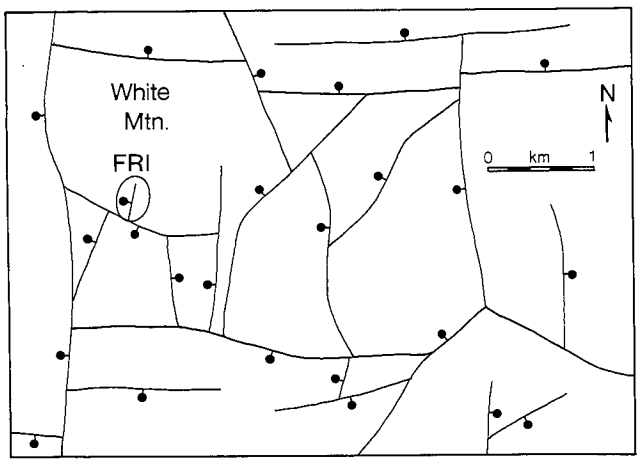

FIGURE 5.—*Map of fault patterns near White Mountain in the Shauntie Hills (after Best and others in press).*

plunges to the north, away from the Tertiary volcanics. Breccia in the fault zone is altered, but could have been altered any time during the volcanic history of the area, 34 to 11 million years ago (Best and others 1984).

The FRI faults formed in an oblique stress field (fig. 6), indicating a possible local perturbation in the regional stress field. Phi is 0.06, so that σ_2 almost equals σ_3. Low phi values have been found in recent borehole experiments by Haimson and Doe (1983), who found that σ_2 and σ_3 were equal down the entire length of a borehole, but that style of faulting changed with depth as σ_1 varied in magnitude and direction. The situation here is similar. There is evidence for a shallow silicic intrusion under the area of figure 5 (Best personal communication 1987). An intrusion would have formed a stress field with oblique principal and shear stresses (Roberts 1970) and caused oblique motion on the FRI faults. Whether or not this intrusion could have formed the orthogonal fault pattern of figure 5 is not known, because other fault surfaces are not exposed and detailed paleostress analysis is impossible.

BLM 1-6a GROUP

Faults of the BLM 1-6 group are in a 1 km^2 area on the east side of Blue Mountain below the Blue Mountain thrust. The data were separated by Angelier's program into two coherent groups that formed in different stress orientations.

The seven faults in the first group were only analyzed by the P-T dihedra and stress tensor methods since the others gave very ambiguous results. P-T and stress tensor results showed an oblique stress field and a phi value of 0.5 (fig. 8). The smallness of the data set, geographical scatter, proximity to a thrust, and oblique stress axes cast some doubts on the reliability of these paleostress analysis results.

BLM 1-6b GROUP

This data set, too, was analyzed only by the P-T dihedra and stress tensor methods (fig. 9). Phi was calculated to be 0.25. The five faults in this group are in the same location as the BLM 1–6a group and carry the same interpretation difficulties. Analysis results show NW–SE extension and NE–SW compression. This orientation will be discussed with the PGR 10 and PGR 16 groups, which have similar orientations.

BLM 7 GROUP

A fault zone in altered carbonate rocks crosses a road a few miles west of Blue Mountain. The twelve recorded faults are mostly oblique and strike slip and resulted from SW–NE extension (fig. 10). The non-verticality of σ_1 is explained by the high value of ϕ (0.76), indicating less distinction between σ_1 and σ_2. Anderson's method is again inadequate to interpret oblique movements and mixed-mode faulting.

This fault zone probably formed in the same NE–SW extensional stress field found by Angelier and others (1985), Barnhard and Anderson (1984), and Zoback and others (1981). They dated this stress field as existing between 17 and 10 Ma.

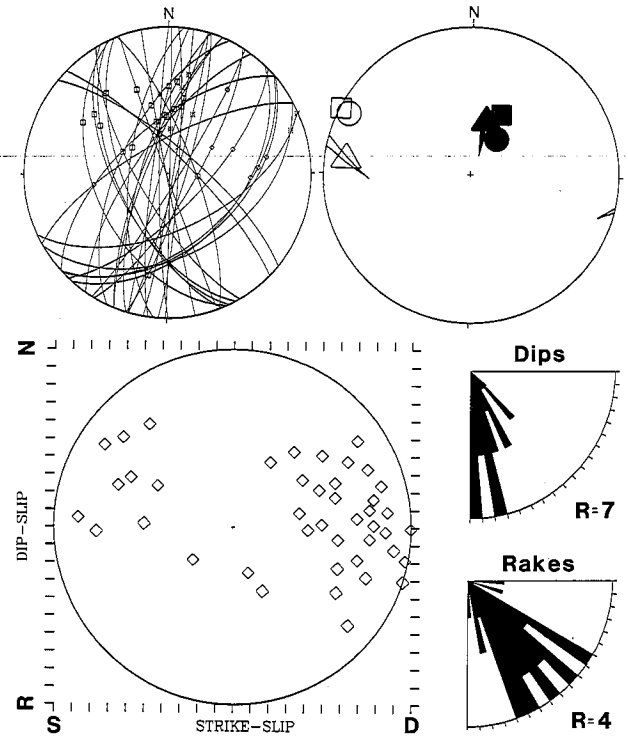

FIGURE 6.—*FRI fault data. Figure 3 caption explains symbols.*

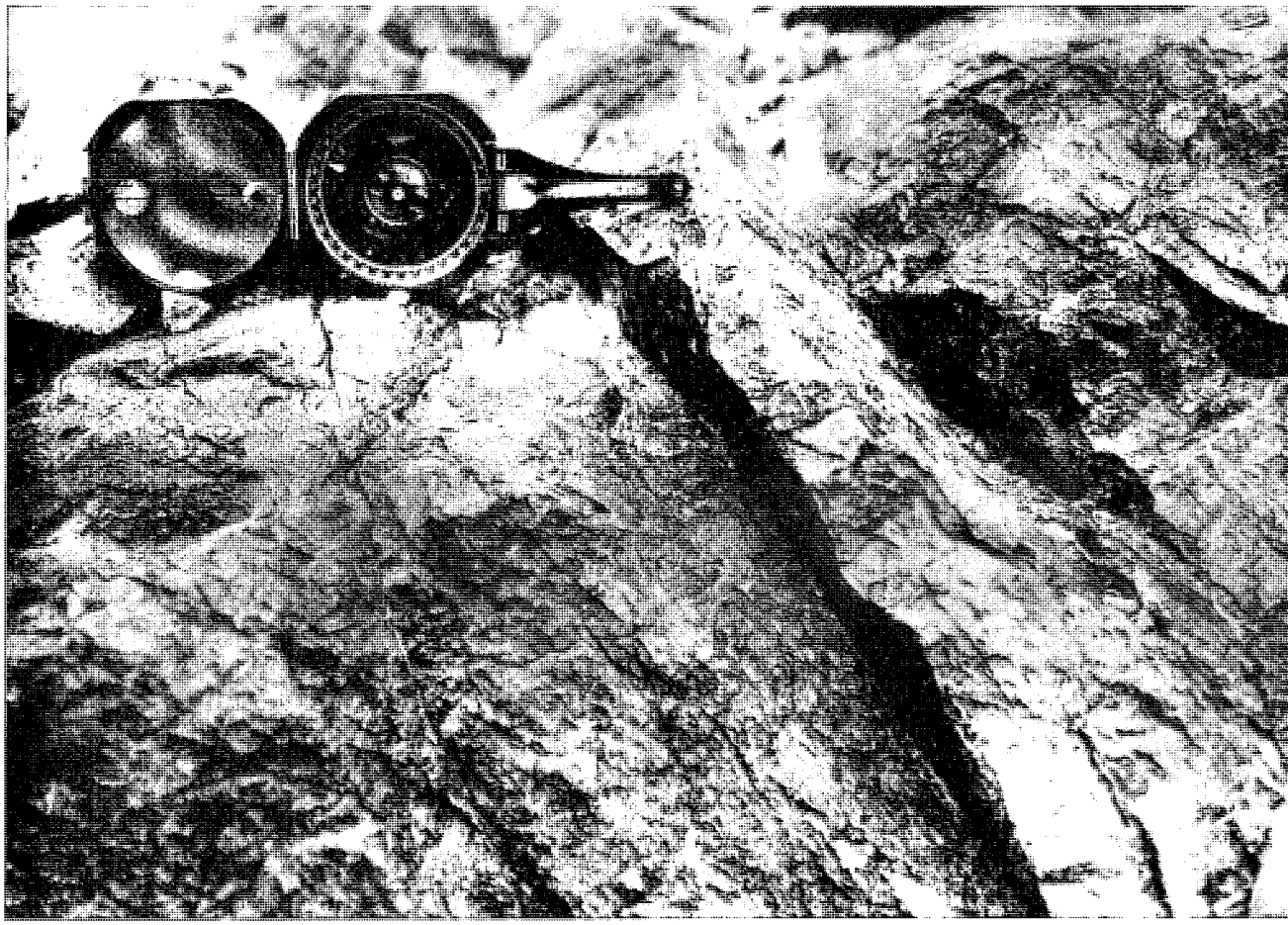

FIGURE 7.—*Typical fault pattern in the FRI fault zone, looking NNE. Note the conjugate normal set and subvertical fault. All rakes are oblique to the north.*

LND GROUP

Another fault zone similar to the FRI group is found in the Lund Quadrangle in an outcrop of Navajo sandstone. The LND group is FRI's mirror image; north-striking faults have slickenlines that plunge to the south away from an east–west-striking normal fault that juxtaposes Mesozoic sandstones and Tertiary volcanic rocks. The mapped normal fault strikes N 45 E, or 30° to 45° from the strikes of measured faults. Faults were recorded along one mile of the mapped fault trace, but the mapped fault surface was never seen.

The 40 faults of this set are all steeply dipping normal and sinistral faults without much geometrical variability (fig. 11). Palinspastic rotation of these faults is geologically impractical for more than 10° of northward tilting, constrained by the dip of the bedrock. Paleostress analyses show NE–SW or NW–SE oblique extension. The value of phi is 1.00, meaning that σ_1 and σ_2 are indistinguishable.

Similarities between this fault set and the FRI set abound, but there is no evidence for a shallow intrusion here (Best personal communication 1987). Oblique motions cannot be explained in terms of reactivation of faults since these faults trend N–S and should have formed in the most recent stress field, which is E–W extension. There is no evidence of a joint system in these rocks parallel to the faults that could have been reactivated under an earlier stress field. Primary fault motions can be oblique, forming in response to local stress field perturbations (Bott 1959). The oblique motions of the LND group could have formed by such a perturbation, possibly caused by movement on the E–W normal fault. These small faults could not be conjugate Riedel shears (Tchalenko 1970) since they strike at such a high angle to the mapped fault. Paleostress results for this group are probably meaningless because either (1) there is not enough geometrical variability in the data set to constrain stress orientations or (2) these faults did not slip independently. In this fault zone it is probably most reliable to take the overall direction of extensional strain across the zone as the extension direction (Zoback and Zoback 1980), namely, southwest.

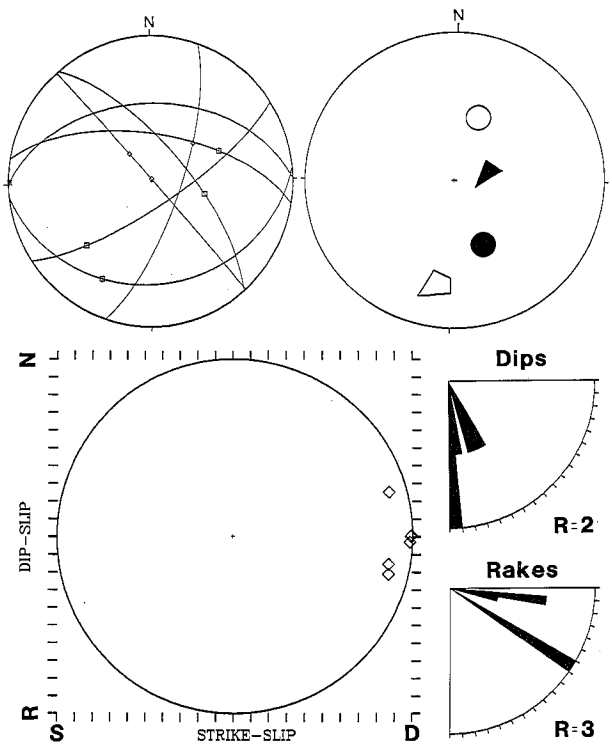

FIGURE 8.—*BLM 1-6a data. Figure 3 caption explains symbols.*

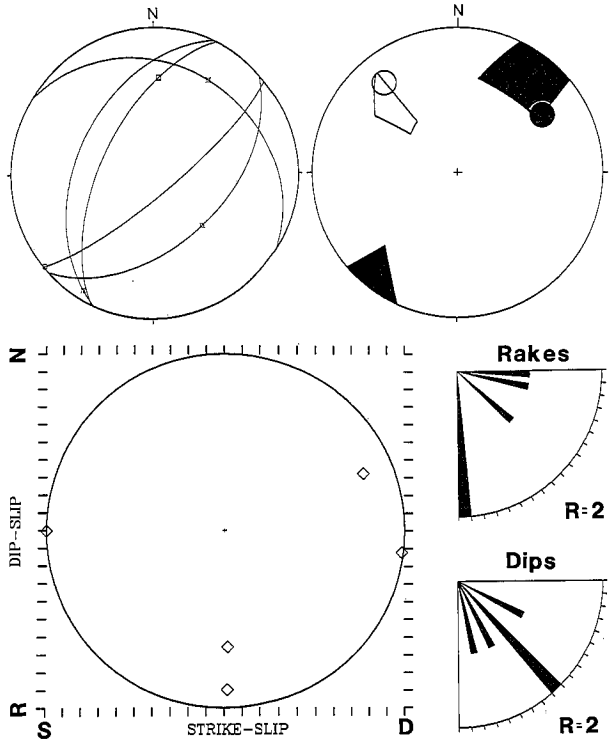

FIGURE 9.—*BLM 1-6b data. Figure 3 caption explains symbols.*

PGR 3 GROUP

The PGR groups of faults are located along three mapped normal faults in Paleozoic quartzites in the central Wah Wah Mountains (fig. 12). Though geographically related, each of these groups represents a different episode of the stress history of the area.

There is an apparent discordance between the stress analysis methods in the PGR 3 dip-slip group (fig. 13). Anderson's and Arthaud's methods indicate east–west extension and a high-angle σ_1. This is because Anderson's does not use the sense of slip on each fault (and combinations thereof) and neither considers magnitude of the intermediate stress. The P-T dihedra method, which accounts for sense of slip but not for varying phi, gives an extension direction of ENE–WSW. The stress tensor method takes these all into account and gives north–south extension and a low value of phi (0.06). Since σ_2 and σ_3 are essentially indistinguishable, the maximum extension direction is in approximate agreement with the other methods at ENE–WSW.

PGR strike-slip faults are a different story (fig. 14). They strike transverse to the normal faults in the same fault zone, and formed in roughly E–W compression. Phi was computed to be 0.49. They are here interpreted as resulting from differential rates of extension within the fault zone. These strike-slip faults are analogous to the "transfer faults" of Gibbs (1984) and Lister and others (1986), and probably formed along pre-existing weaknesses that were suitably oriented. Movement on the normal faults "pushed" the transfer faults, giving them an apparent stress orientation directly opposite to that of the normal faults that caused their motion. This relation will later be shown to be significant. Thus it is evident that fault geometries can create local fault motions geometrically related to the regional stress field. Because one criterion of paleostress analysis is independence of faults, the results of all methods would be meaningless and are not presented here.

PGR 5 GROUP

The 11 dip-slip and 13 strike-slip faults of the PGR 5 group represent possibly the oldest determinable orientation of the stress field in the study area. The transfer fault phenomenon is not apparent here, but faults are divided between dip and strike slip for clarity (figs. 15 and 16). The P-T dihedra and stress tensor methods give coherent results of north–south extension with σ_1 near vertical for both sets of faults. Anderson's method gave the same results for the dip-slip faults, but was again thrown off by oblique movements and senses of slip in the

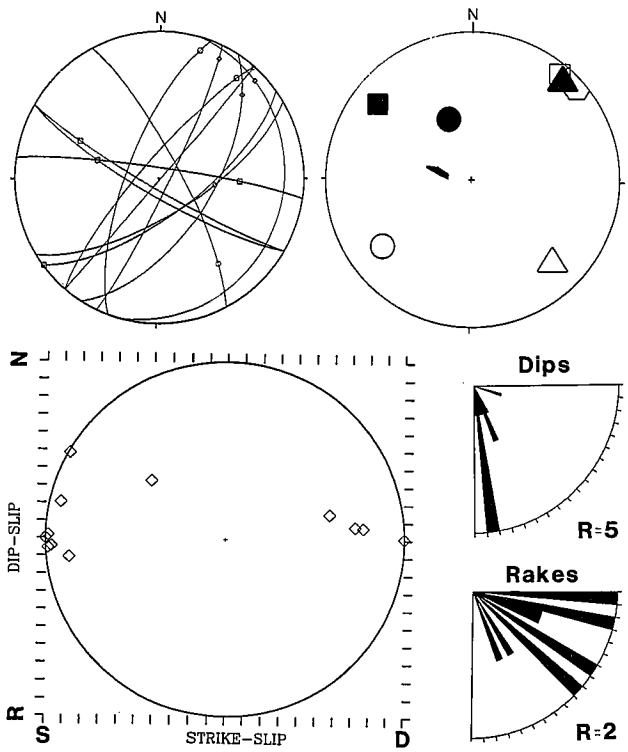

FIGURE 10.—*BLM 7 data. Figure 3 caption explains symbols.*

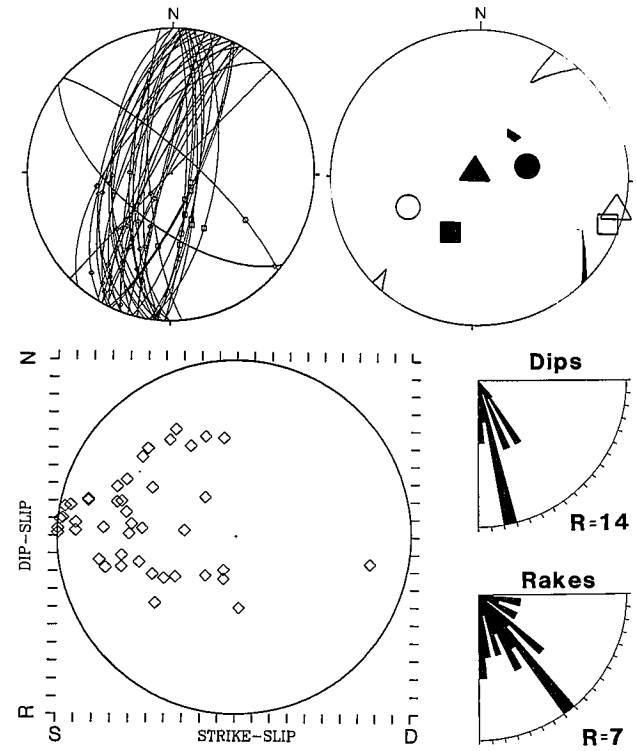

FIGURE 11.—*LND data. Figure 3 caption explains symbols.*

strike-slip set (fig. 16). Arthaud's method had the opposite effect—good results for the strike-slip set and poor results for the dip-slip set. This was due to scatter of strikes in the dip-slip set, so that M-pole plots scattered widely over the stereo net and caused ambiguous contouring problems.

One and a half miles north of these faults is an igneous dike dated at between 23 and 20 million years (Keith and others in press) that trends east–west. Farther north and west and in the northern Star Range are more groups of dikes of the same age with the same trend (Best and others 1984, Best and others in press), indicative of north–south extension. Due to proximity of the dikes and the large and coherent data set here, it is assumed that the PGR 5 faults represent the same stress field that formed the igneous dikes, and the early Miocene age is also assigned to the faults.

PGR 10 GROUP

PGR 10 faults are a curious mixture of 4 dextral, 4 sinistral, and 1 reverse fault (fig. 17). The P-T dihedra and stress tensor methods again agree, showing a slightly oblique stress field of WNW–ESE extension and NE–SW compression. The value of phi (0.5) indicates strong distinction between stress axis magnitudes. Because Anderson's method does not deal with oblique rake angles, it gives an apparently simple answer of N–S extension and E–W compression, somewhat like the transfer faults of PGR 3. Arthaud's method suffers the same malady, even though it is free from stress axis-fault plane angle restrictions.

The oblique stress axes determined by the stress tensor method resulted from the lack of conjugate fault control or wider scatter of strikes to tie down a stress axis orientation. This is a weakness in the method. The P-T dihedra method, which treats faults individually, is the most reliable in this case.

The age of these faults is equivocal. NW–SE extension can be inferred in the region from orientations of igneous dikes dated at 23–18 million years (Best and others 1984), but this conflicts with findings of this paper (PGR 5 group), Zoback and others (1981)—who dated ENE–WSW extension at between 20 and 10 million years—Best and others (in press), and Best and others (1987). The dikes could have intruded along older joints, or the faulting episode could have been exceptionally brief at about 20 Ma. or pre–23 Ma. The pre-north–south extension scenario (pre–23 Ma.) is preferred because it presents fewer complications in a tectonic explanation, but more study is needed.

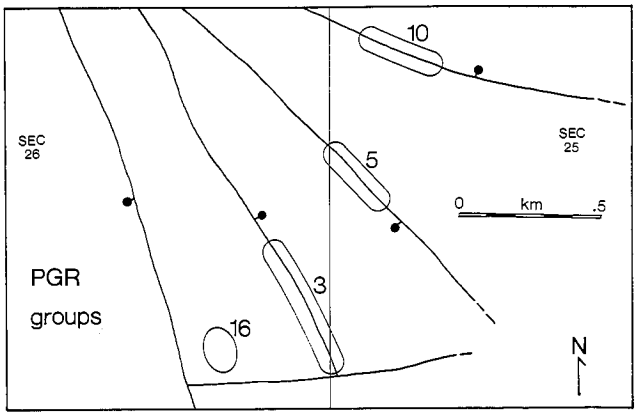

FIGURE 12.—*Map showing relative locations of PGR fault zones (after Abbott and others 1983).*

PGR 16 GROUP

All four paleostress methods agree on NW–SE extension for the PGR 16 group (fig. 18). In performing Anderson's and Arthaud's methods, the "missing" conjugate fault set had to be assumed. In the stress tensor method, this lack of conjugate control caused the statistical mean of predicted and actual slip directions to rise, but in this case had just enough control to give coherent results. Phi is 0.8, which means σ_2 is almost equal to σ_1. These faults represent the same stress field orientation as the PGR 10 group, NW–SE extension, and could correspond to NE–SW-striking igneous dikes nearby.

STM GROUP

STM faults are located a few miles south of Steamboat Mountain in the southern Needle Range. They are in Tertiary volcanic rocks in a small fault zone 10 meters long, and form a coherent plot (fig. 19). They formed under ENE–WSW extension according to each method, with a 0.57 phi value. The coherence and simplicity of this fault set make stress solutions straightforward for each method, although conjugate faults must be assumed for Anderson's and Arthaud's methods. Strikes are diverse enough that the stress tensor method gave reliable results without actual conjugate pairs. These faults probably formed early in Basin and Range history, between 20 and 10 Ma., during NE–SW extension that dominated the region (Zoback and others 1981).

BIB GROUP

The Bible Spring fault zone is a major fault with vertical offset of approximately 1 km, and was active between 22 and 12 million years ago (Best and others 1987). Horizontal offset has not been determined. The fault can be traced for about 50 kilometers, although best exposures are near

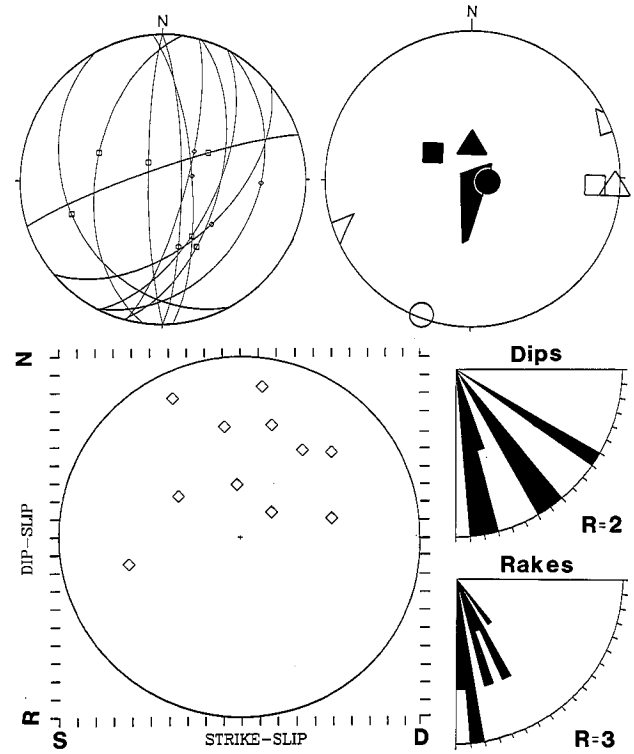

FIGURE 13.—*PGR 3 dip-slip data. Figure 3 caption explains symbols.*

Bible Spring in the southernmost Needle Range. Some slickenlines recorded here are from a surface 150 meters long and up to 3 meters high (fig. 20). Although the data set is small (only 5 faults), weighting for the stress tensor analysis according to displacement makes the set equivalent to 21 faults of the size discussed in most sets above, which averaged only a few centimeters displacement.

The P-T dihedra and stress tensor methods again agree closely (fig. 21), whereas the other two methods are slightly biased by oblique rake angles. This result of NNW–SSE extension and ENE–WSW compression is curious in terms of placing it in the context of Miocene Basin and Range tectonics. Zoback and others (1981) have shown that NE–SW extension was active at this time. As mentioned above, transfer faults can give apparent, but erroneous, paleostress results opposite to those of their parent normal faults. This is apparently the case with the Bible Spring fault zone. As regional normal faulting initiated in early Miocene, the BSFZ acted as a transfer fault, separating extending areas to the north from less-extended areas to the south, much like the Garlock Fault (Davis and Burchfiel 1973). It is not known whether it formed earlier as a normal fault or whether the dip-slip component is simply a result of oblique slip, since slickensides record only the last motion; however, data from Best

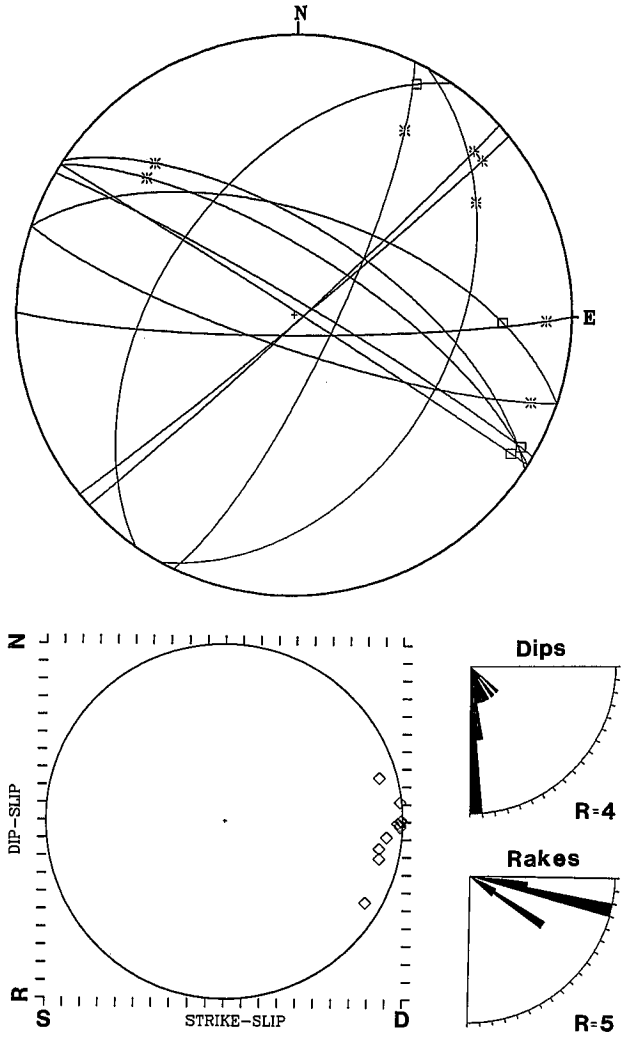

FIGURE 14.—*PGR 3 strike-slip data. Figure 3 caption explains symbols. Paleostress analyses are not shown (see text).*

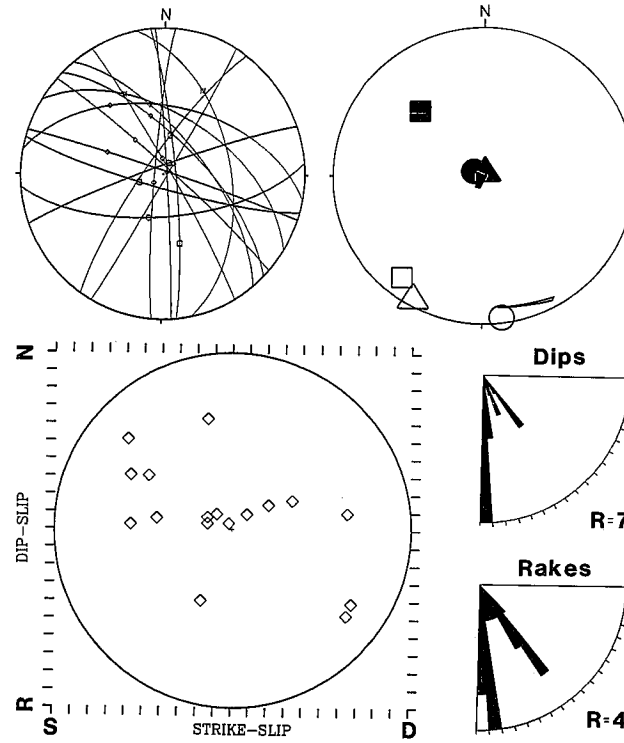

FIGURE 15.—*PGR 5 dip-slip data. Figure 3 caption explains symbols.*

and others (1984) suggest that the southwestern segment of the BSFZ is a reactivation of early Miocene normal faults, which were not reactivated to the northeast in the Wah Wah Mountains.

SLIP MODEL

The slip model of Reches (1983) predicts fault patterns with orthorhombic symmetry. Such symmetry is seen in the BIB fault group, but this is probably a reactivated fault and thus fails to qualify. Another possible location is near the FRI fault zone (fig. 5). The fault pattern here is much like the "zigzag" pattern in Reches (1983, fig. 8) and could represent true orthorhombic symmetry. This could be confirmed by examination of each of the strikes, dips, and slickenlines of each of these faults, but they are very poorly exposed.

Orthorhombic symmetry is not found elsewhere in the study area. This could be due to the complex stress history of the area, which would have masked traces of such an intricate fault geometry, or to the lack of suitably oriented pre-existing planes on which to fully develop the pattern.

STRESS FIELD ROTATION

ROTATION STAGES

Stress field rotations in the Basin and Range have been discussed by Zoback and others (1981), who found a 45° clockwise rotation during the past 10 million years in Nevada. Angelier and others (1985) found a 65° Neogene clockwise rotation at Hoover Dam, but they also indicated possible rotation of the rock body.

The regional stress field has rotated at least 90° in stages (fig. 22), from N–S extension between 23 and 20 million years ago (this paper, PGR 5 faults) to the present E–W extension in this region (Zoback and Zoback 1980). The intermediate NE–SW extension direction is shown by the BLM 7, PGR 3, STM, and BIB faults. NNE–WSW extension was found by Zoback and others (1981), who dated it at between 20 and 10 million years based on igneous dikes and sedimentation. The NE–SW extension

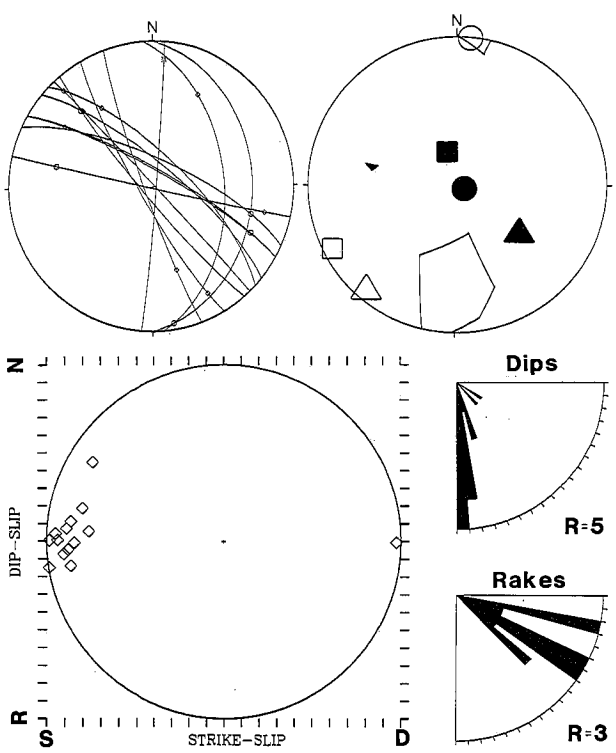

FIGURE 16.—*PGR 5 strike slip. Figure 3 caption explains symbols.*

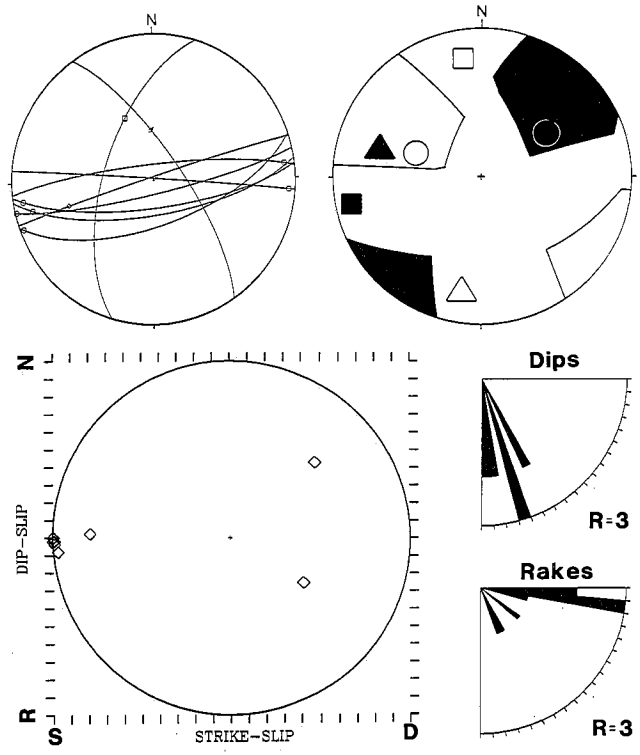

FIGURE 17.—*PGR 10 data. Figure 3 caption explains symbols.*

found in the study area is probably a local variation in this same stress field, and is constrained to between 22 and 12 million years by the age of the Bible Spring fault zone. The most recent stage of roughly E–W extension is shown in the MIL and FRI groups, although the FRI group was influenced by other forces. The NW–SE extension directions of the BLM 1-6b, PGR 10, and PGR 16 groups are equivocal because of conflicting data, but could represent a pre- or early Miocene event.

FAULT REACTIVATION

The large number of oblique faults in the study area is probably best explained by activation of pre-existing fractures, but there are several important exceptions. Faults of the PGR groups represent extension directions of NW–SE, N–S, and NE–SW, which probably range in age from earliest to mid-Miocene. Although the earliest-formed faults were suitably oriented for reactivation in the later stress fields (Raleigh and others 1972), no reactivation is seen. This could be because the faults have relatively minor displacements (a few meters total). But whatever the reason, it is important to note that not all suitably oriented faults are active during the latest faulting episode. This contrasts sharply with assumptions of Angelier (1979, 1984), Arthaud (1969), Bott (1959), and others. Reactivation of faults is especially likely in an area such as this where multiple faulting events have occurred, as seen in the Bible Spring fault zone, and in east–west faults of the Mineral Range near Milford that are seismically active and may be reactivated faults (Nielson and others 1986), but this is apparently not an inviolable rule.

FAULT KINEMATICS

An interesting geometry produced by transfer faulting is alternating dextral and sinistral faults (fig. 23). These faults outline blocks that shuffle past each other as extension proceeds irregularly. This geometry causes apparent conflicts when analyzing paleostress, because these faults represent conflicting stress orientations. Such problems can only be resolved by careful field identification of transfer faults. It must be emphasized that paired sinistral and dextral faults do not necessarily represent actual conflicting stress regimes, but rather are a result of shuffling of blocks during extension, at times reversing displacement on some lateral block boundaries. A feature that could be added to future paleostress analysis methods, then, is the ability to deal with non-independent faults,

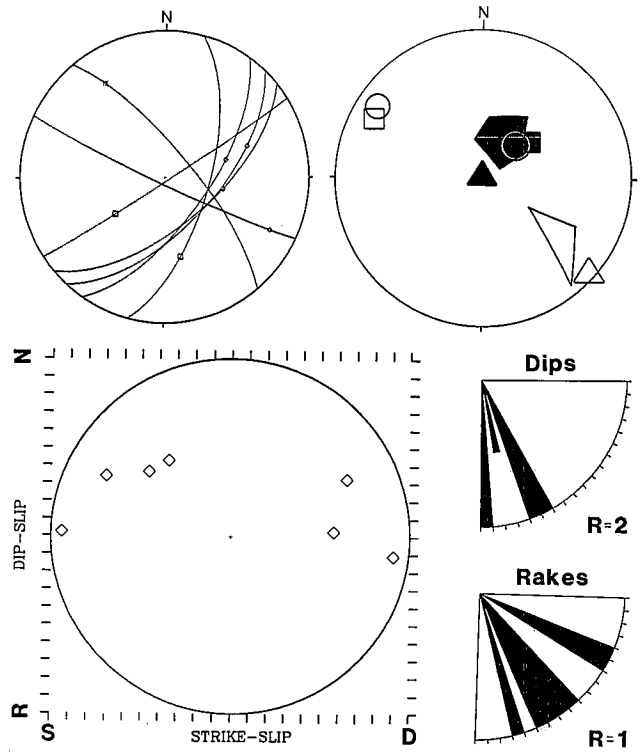

FIGURE 18.—*PGR 16 data. Figure 3 caption explains symbols.*

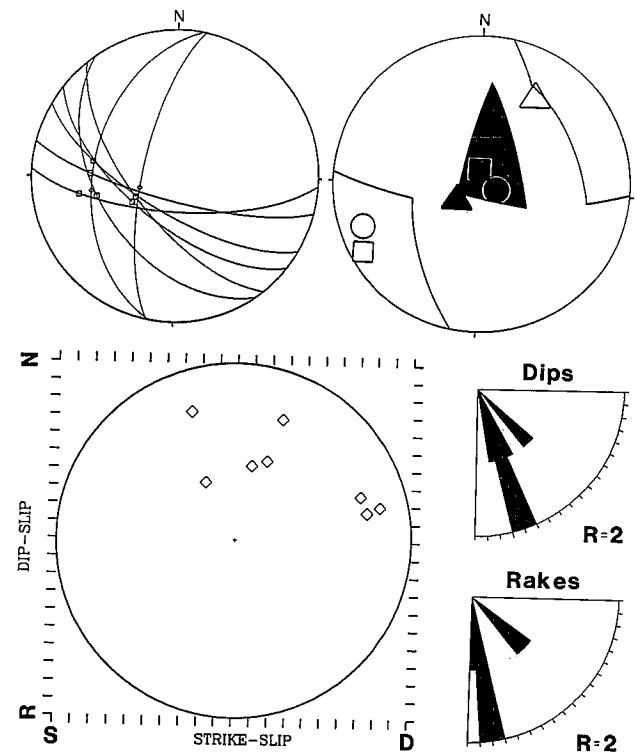

FIGURE 19.—*STM data. Figure 3 caption explains symbols.*

such as transfer faults, and use their slip directions in conjunction with their parent normal faults as an added constraint on total strain in the fault system.

Another feature of transfer faults within fault zones is the independence of their rake angles from the dips of the normal faults that apparently caused them. For example, there is no correlation between the dip distribution of PGR 3 normal faults and the rake distribution of PGR 3 strike-slip faults (fig. 13D and 14D). Motion on these faults must, therefore, be more complicated. On a larger scale, low rake angles probably result from extension along lystric normal faults that flatten into a subhorizontal surface at depth. Within a fault zone, however, different amounts of displacement or slightly different normal fault dips on either side of a transfer fault can form low-angle slickenlines when both sides move simultaneously.

CONCLUSIONS

Faulting in the study area ranges in age from early Miocene to Quaternary, and probably represents 135° of clockwise rotation of the stress field from NW–SE extension to E–W extension. The earliest stress field is probably the NW–SE extension, but conflicting data need to be resolved. A distinct phase of N–S extension between 23 and 20 Ma. was found in a large and coherent group of faults that formed near E–W-striking igneous dikes of that age. This period is also manifest in topographic barriers to distribution of volcanic rocks and E–W igneous dikes (Best and others 1984, Best and others in press). The younger NE–SW extension is the most common in the study area. The Bible Spring fault zone acted as a transfer fault during that time, separating extended areas to the north from less extended areas to the south, like the Garlock Fault. NE–SW extension was active at least late in the 22–12 Ma. activity of the Bible Spring fault zone. The youngest faults in the area were produced by E–W extension, which is active today.

The clockwise stress field rotation corresponds in time with progressive development of the dextral San Andreas transform (Atwater 1970), but distributed dextral shear fails to account for the many subregional stress field variations in the Great Basin (Sbar 1982) and the spatial and chronological development of Basin and Range faulting (Eaton 1979). Models envisaging a simple spreading mantle plume (Dickinson and Snyder 1979) cannot easily account for a rotating stress field unless regional variations are considered. Such regional and chronological stress field variations require local sources (Sbar 1982). The spreading mantle plume/subducted slab window model also fails to account for timing and location of Basin and Range fault development. The extent of the NW–SE

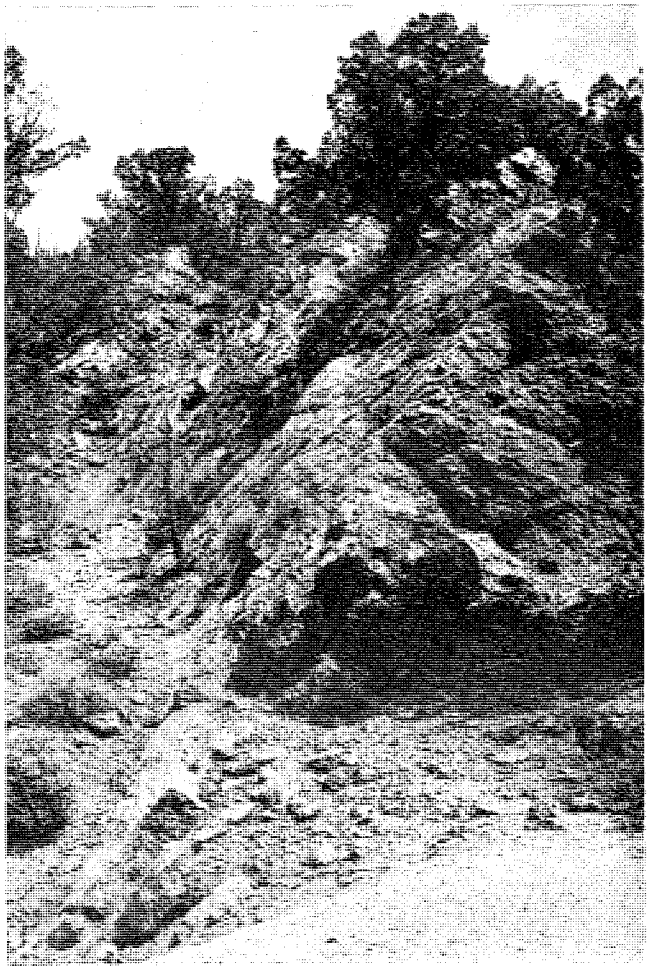

FIGURE 20.—*Silicified volcanic rocks of the Bible Spring transfer fault. Scarp is 3 meters high and is almost entirely highly polished and striated.*

and N–S extensional events must now be determined, and these events must be considered in future tectonic interpretations of the Great Basin.

Anderson's method of paleostress determination is useful in only the most simple cases, and is especially prone to error in cases of oblique faulting. Arthaud's method is less restricted by angles between faults and stresses, but fails to fully account for slip senses, reactivated fault orientations, and mixed modes. The P-T dihedra and stress tensor methods account for slip senses above and beyond the other methods, and give reliable results in even complex fault groups. The P-T dihedra method has the singular advantage of treating faults individually without regard to conjugate mates. The stress tensor method also allows separations of data into subgroups of coherent faulting events, and computes the value of ϕ—very useful features. In mixed, large, or complex data sets, Angelier's stress tensor method is the most versatile of the four methods.

The slip model of Reches (1983) seems to apply to simple cases such as faulting around White Mountain, but seems not to apply generally to preserved faults in the study area. The stress history of this area is too complex for the intricate orthorhombic symmetry to be preserved with any regularity.

Slickenlines are the major key to determining paleostress orientations in complexly faulted areas like this one. Paleostress methods that do not consider deviatoric stresses and fault reactivation often give inaccurate results. It is critical that the correct sense of slip be ascribed to each fault and that careful fieldwork establish the complete faulting picture in an area. Failure to identify transfer faults will result in erroneous paleostress results.

ACKNOWLEDGMENTS

This research was funded in part by ASBYU and a BYU Geology Department research grant to Drs. Myron Best and Bart Kowallis. Thanks to the U.S. Geological Survey, Ernie Anderson, and Ted Barnhard for use of computer facilities and generous technical assistance, and to Myron Best, Bart Kowallis, Ernie Anderson, Jacques Angelier, and Greg Davis for stimulating discussions. Interpretations herein are, however, my own.

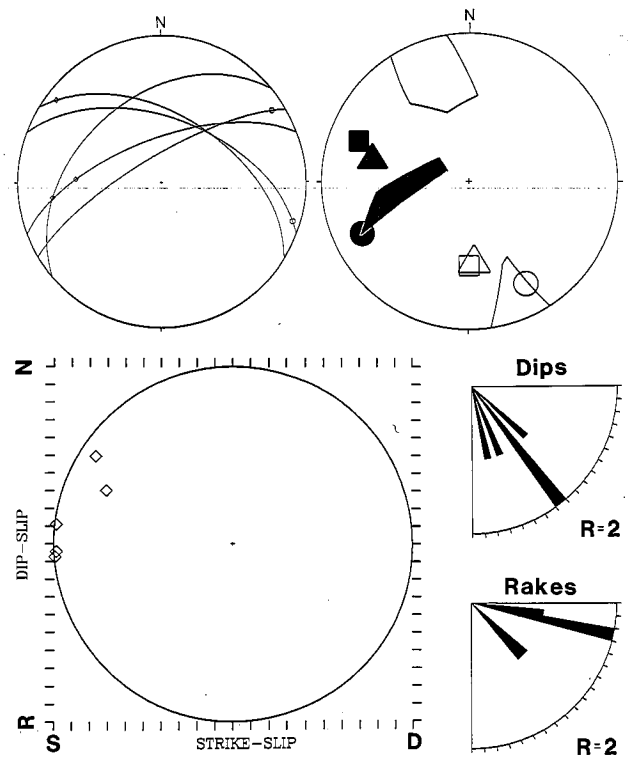

FIGURE 21.—*BIB data. Figure 3 caption explains symbols.*

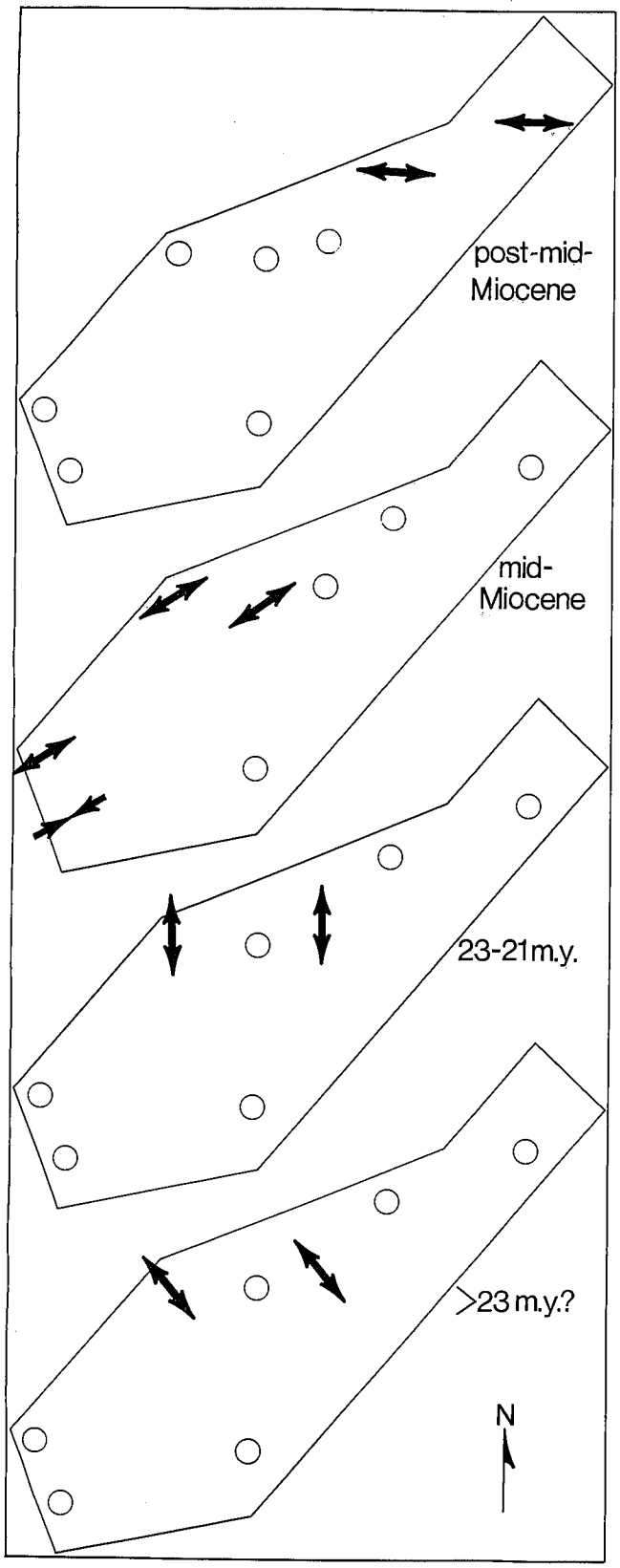

FIGURE 22.—*Summary of paleostress analyses. Outlined area is study area (see fig. 1). Arrows indicate principal extension directions (σ_3). Arrows on BIB location point inward since BIB is a transfer fault (see text). Circles are fault zone locations.*

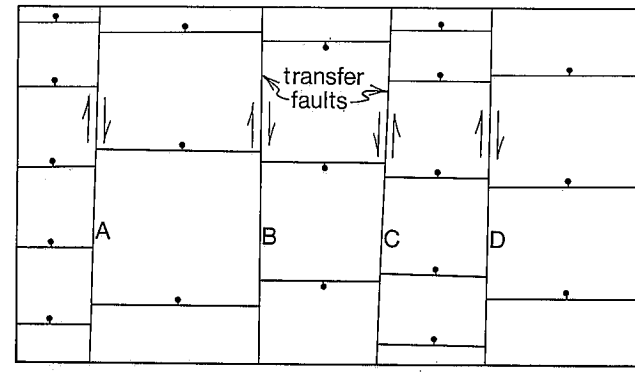

FIGURE 23.—*Idealized representation of transfer fault geometry. Scale is arbitrary, but here represents one fault zone. Three en echelon normal faults strike left–right across the diagram. Transfer faults A, B, C, and D accommodate differential rates of extension caused either by reversal of fault polarity (B and C) or different amounts of extension (A and D). Note alternating sense of slip between faults B and D.*

REFERENCES CITED

Abbott, J. T., Best, M. G., and Morris, H. T., 1983, Geologic map of the Pine Grove–Blawn Mountain area, Beaver County, Utah: U.S. Geological Survey Miscellaneous Investigations Series Map I-1479.

Anderson, E. M., 1951, The Dynamics of Faulting: Oliver and Boyd, Edinburgh, 206p.

Anderson, R. E., 1984, Strike-slip faults associated with extension in and adjacent to the Great Basin: Geological Society of America Abstracts with Programs 16 (6), p. 429.

Anderson, R. E., and Barnhard, T. P., 1984, Late Cenozoic fault and fold patterns in Sevier County, Utah, and their relationship to seismicity in the area: Geological Society of America Abstracts with Programs 16 (6), p. 430.

Angelier, J., 1979, Determination of the mean principal directions of stresses for a given fault population: Tectonophysics, v. 56, T17–T26.

———, 1984, Tectonic analysis of fault slip data sets: Journal of Geophysical Research, v. 89, no. B7, p. 5835–48.

Angelier, J., Colletta, B., and Anderson, R. E., 1985, Neogene paleostress changes in the Basin and Range: A case study at Hoover Dam, Nevada-Arizona: Geological Society of America Bulletin, 96 (3), p. 347–61.

Angelier, J., and Mechler, P., 1977, Sur une methode graphique de recherche des contraintes principales egalement utilisable en tectonique et en seismologie: La methode des diedres droits: Bull. Soc. Geol. Fr., XIX(7), p. 1309–18.

Arthaud, F., 1969, A graphic method of determination of the shortening, elongation, and intermediate directions from a population of faults: Extant de Bulletin de la Societe geologique de France, 7 e Serie, t. 11, p. 720–37.

Atwater, T., 1970, Implications of plate tectonics for the Cenozoic tectonic evolution of western North America: Geological Society of America Bulletin, v. 81, p. 3513–36.

Baer, J. L., 1962, Geology of the Star Range, Beaver County, Utah: Brigham Young University Geology Studies, v. 9, pt. 2, p. 29–52.

Barnhard, T. L., and Anderson, R. E., 1984, Extensional and compressional paleostress states in the western Colorado Plateau, central Utah: Geological Society of America Abstracts with Programs 16 (6), p. 437.

Best, M. G., Lemmon, D., and Morris, H. T., in press, Geologic map of the Frisco and Milford Quadrangles, Beaver County, Utah: U.S. Geological Survey Miscellaneous Investigations Series map.

Best, M. G., Mehnert, H. H., Keith, J. D., and Naeser, C. W., 1984, Miocene magmatism and tectonism in and near the southern Wah Wah Mountains, southwestern Utah: U.S. Geological Survey Professional Paper 1433B.

Best, M. G., Morris, H. T., Kopf, R. W., and Keith, J. D., 1987, Geologic map of the southern Pine Valley area, Beaver and Iron Counties, Utah: U.S. Geological Survey Miscellaneous Investigation Series Map I-1794.

Bott, M. H. P., 1959, The mechanisms of oblique slip faulting: Geological Magazine, v. 96, p. 109–17.

Bruhn, R. L., and Pavlis, T. L., 1981, Late Cenozoic deformation in the Matanuska Valley, Alaska: Three-dimensional strain in a forearc region: Geological Society of America Bulletin, v. 92, pt. 1, p. 282–93.

Davis, G. A., and Burchfiel, B. C., 1973, Garlock fault: An intra-continental transform structure, southern California: Geological Society of America Bulletin, v. 84, p. 1407–22.

Dickinson, W. R., and Snyder, W. S., 1979, Geometry of subducted slabs related to San Andreas transform: Journal of Geology, v. 87, p. 609–27.

Eaton, G. P., 1979, A plate-tectonic model for crustal spreading in the western United States: In Riecker, R. E. (ed.), Rio Grande Rift: Tectonics and Magmatism: American Geophysical Union, Washington, D.C., p. 7–32.

Gibbs, A. D., 1984, Structural evolution of extensional basin margins: Geological Society of London Journal, v. 141, p. 609–20.

Grant, S. K., and Best, M. G., 1979, Geologic map of the Lund Quadrangle, Iron County, Utah: U.S. Geological Survey Open-File Report 79-1655.

Haimson, B. C., and Doe, T. W., 1983, State of stress, permeability, and fractures in the Precambrian granite of northern Illinois: Journal of Geophysical Research, v. 88, no. B9, p. 7355–71.

Keith, J. D., Shanks, W. C., III, Archibald, D. A., and Farrar, E., in press, Volcanic and intrusive history of the Pine Grove porphyry molybdenum system, southwestern Utah.

Lister, G. S., Etheridge, M. A., and Symonds, P. A., 1986, Detachment faulting and the evolution of passive continental margins: Geology, v. 14, p. 246–50.

McKenzie, D. P., 1969, The relationship between fault plane solutions for earthquakes and the directions of the principal stresses: Bulletin of the Seismological Society of America, v. 59, p. 591–601.

Nielson, D. L., Evans, S. H., Jr., and Sibbett, B. S., 1986, Magmatic, structural, and hydrothermal evolution of the Mineral Mountains intrusive complex, Utah: Geological Society of America Bulletin, v. 97, p. 765–77.

Paterson, M. S., 1958, Experimental deformation and faulting in Wombeyan marble: Geological Society of America Bulletin, v. 69, p. 465–76.

Raleigh, C. B., Healy, J. H., and Bredehoeft, J. D., 1972, Faulting and crustal stress at Rangely, Colorado: In Heard, H. C., and others (eds.), Flow and Fracture of Rocks: Geophysical Monograph Series, v. 16, American Geophysical Union, Washington, D.C., p. 275–84.

Reches, Z., 1983, Faulting of rocks in three-dimensional strain fields. II. Theoretical analysis: Tectonophysics, v. 95, p. 133–56.

Roberts, J. L., 1970, The intrusion of magma into brittle rocks: In Newall, G., and Rast, N. (eds.), Mechanism of Igneous Intrusion: Liverpool, Gallery Press, p. 287–338.

Sbar, M. L., 1982, Delineation and interpretation of seismotectonic domains in western North America: Journal of Geophysical Research, v. 87, p. 3919–28.

Tchalenko, J. S., 1970, Similarities between shear zones of different magnitudes: Geological Society of America Bulletin, v. 81, p. 1625–40.

Zoback, M. L., and Zoback, M., 1980, State of stress in the conterminous United States: Journal of Geophysical Research, v. 85, no. B11, p. 6113–56.

Zoback, M. L., Anderson, R. E., and Thompson, G. A., 1981, Cainozoic evolution of the state of stress and style of tectonism of the Basin and Range Province of the western United States: Royal Society of London, Philosophic Transactions, series A, v. 300, no. 1454, p. 407–34.